Clinical Cancer Research

Clinically Viable Gene Expression Assays with Potential for Predicting Benefit from MEK Inhibitors

Roz Brant[1], Alan Sharpe[2], Tom Liptrot[3], Jonathan R. Dry[4], Elizabeth A. Harrington[2], J. Carl Barrett[5], Nicky Whalley[6], Christopher Womack[7], Paul Smith[6], and Darren R. Hodgson[1]

Abstract

Purpose: To develop a clinically viable gene expression assay to measure RAS/RAF/MEK/ERK (RAS–ERK) pathway output suitable for hypothesis testing in non–small cell lung cancer (NSCLC) clinical studies.

Experimental Design: A published MEK functional activation signature (MEK signature) that measures RAS–ERK functional output was optimized for NSCLC *in silico*. NanoString assays were developed for the NSCLC optimized MEK signature and the 147-gene RAS signature. First, platform transfer from Affymetrix to NanoString, and signature modulation following treatment with *KRAS* siRNA and MEK inhibitor, were investigated in cell lines. Second, the association of the signatures with *KRAS* mutation status, dynamic range, technical reproducibility, and spatial and temporal variation was investigated in NSCLC formalin-fixed paraffin-embedded tissue (FFPET) samples.

Results: We observed a strong cross-platform correlation and modulation of signatures *in vitro*. Technical and biological replicates showed consistent signature scores that were robust to variation in input total RNA; conservation of scores between primary and metastatic tumor was statistically significant. There were statistically significant associations between high MEK ($P = 0.028$) and RAS ($P = 0.003$) signature scores and *KRAS* mutation in 50 NSCLC samples. The signatures identify overlapping but distinct candidate patient populations from each other and from *KRAS* mutation testing.

Conclusions: We developed a technically and biologically robust NanoString gene expression assay of MEK pathway output, compatible with the quantities of FFPET routinely available. The gene signatures identified a different patient population for MEK inhibitor treatment compared with *KRAS* mutation testing. The predictive power of the MEK signature should be studied further in clinical trials. *Clin Cancer Res; 23(6); 1471–80. ©2016 AACR.*

See related commentary by Xue and Lito, p. 1365

Introduction

KRAS mutations are observed in approximately 26% and 11% of non–small cell lung cancer (NSCLC) adenocarcinomas in Western and Asian populations, respectively (1, 2). Although this segment of NSCLC is viewed as a high unmet clinical need, the prognostic and predictive value of *KRAS* mutations is unclear (3, 4). Consistent with the hypothesis that the RAS/RAF/MEK/ERK (RAS–ERK) pathway is important in *KRAS*-mutant tumors, clinical activity has been demonstrated with the combination of docetaxel and the MEK inhibitor (MEKi) selumetinib (AZD6244, ARRY-142886) in patients with *KRAS*-mutant advanced NSCLC as second-line treatment (5). However, trametinib, another MEKi, has shown comparable response rates in patients with *KRAS* mutation not detected and *KRAS*-mutant NSCLC in combination with docetaxel, indicating a sensitive patient population outside the *KRAS*-mutant segment (6). It is therefore possible that *KRAS* status is an imperfect predictor of RAS–ERK pathway dependence and/or a level of pathway dependence is conferred upon the tumor by docetaxel irrespective of *KRAS* mutation status. Furthermore, *KRAS* mutation status alone is unlikely to encapsulate the diverse pathway signaling dependence of NSCLC tumors. For instance, elevated RAS–ERK signaling can be driven by mechanisms including mutations in *BRAF, HRAS,* and other canonical RAS–ERK pathway components; receptor tyrosine kinase activation; and deletion of GTPase-activating proteins (7). Hence, it is possible that a measurement of RAS–ERK pathway activity, independent of the point of genetic activation, may represent a more effective strategy for personalized medicine.

In 2010, two publications reported gene expression signatures associated with activating *KRAS* mutations/RAS–ERK pathway activation (8, 9). The 147-gene Loboda and colleagues signature ("RAS signature") was designed to predict the totality of *KRAS* signaling and was derived from interrogating gene expression in

[1]Translational Science, Oncology iMED, AstraZeneca, Macclesfield, UK. [2]Oncology iMED, AstraZeneca, Cambridge, UK. [3]Informatics, The Christie NHS Foundation Trust, Manchester, UK. [4]iScience, Oncology iMED, AstraZeneca, Waltham, Massachusetts. [5]Translational Science, Oncology iMED, AstraZeneca, Waltham, Massachusetts. [6]Cancer Biosciences, AstraZeneca, Cambridge, UK. [7]Histologix Ltd, Nottingham, UK.

Note: Supplementary data for this article are available at Clinical Cancer Research Online (http://clincancerres.aacrjournals.org/).

T. Liptrot and C. Womack are former employees of AstraZeneca.

Corresponding Author: Darren R. Hodgson, AstraZeneca, Alderley Park, Macclesfield, Cheshire, SK10 4TG, UK. Phone: 44-1625-516105; Fax: 44-1625-516105; E-mail: Darren.Hodgson@astrazeneca.com

doi: 10.1158/1078-0432.CCR-16-0021

Translational Relevance

Gain-of-function mutations in *KRAS* and *BRAF* activate the RAS/RAF/MEK/ERK (RAS–ERK) signaling pathway and have been used to select patients with non–small cell lung cancer (NSCLC) or melanoma suitable for MEK inhibitor targeted therapy. RAS–ERK signaling can also be driven by a number of other genetic variants, including those in other RAS pathway components, receptor tyrosine kinase activation, and deletion of GTPase-activating proteins. Gene expression signatures that measure pathway dependence may represent an alternative patient selection strategy to single gene mutation detection methods. We have systematically addressed the technical and biological prerequisites to clinical hypothesis testing for two published gene expression signatures. The resulting assay, using NanoString nCounter technology, can be used on formalin-fixed paraffin-embedded tissue samples, which represent the format, quantity, and quality routinely available from patients with NSCLC. This assay suggests an alternative MEK inhibitor–sensitive population for hypothesis testing in clinical trials.

lung, breast, and colon cancer datasets. The transcriptional readout was suggested to be superior to *KRAS* status as a predictor of RAS–ERK pathway dependence and predictive of sensitivity to MEKi. The Dry and colleagues 18-gene signature ("MEK signature") captured signaling exclusively from MEK and was able to stratify MEK pathway activation and/or MEKi sensitivity in lung, breast, colon, and melanoma cell lines and xenograft models. Dry and colleagues also described a 13-gene signature ("CRes signature") linked to MEK-independent RAS signaling and resistance to MEKi. Both gene signatures were developed *in silico* from pan-cancer datasets generated from microarray measurements of frozen tumor samples or cell lines.

The application of microarrays for clinical investigation is compromised by cost, reproducibility, failure rate, and preanalytical requirements for tumor tissue quantity and quality (10, 11). Thus, there is a fundamental need to transfer gene signatures to a platform capable of robustly profiling small amounts of RNA extracted from formalin-fixed paraffin-embedded tissue (FFPET), the typical clinical sample type. Furthermore, consistent scores on repeat testing are imperative across technical variables such as RNA input, reagent batch, and selection of a representative area of tissue for testing.

In addition to a technically validated assay, a valid biomarker hypothesis is required. To be a successful predictive biomarker, gene signature profiles should be consistent within a tumor sample such that multiple testing would elicit the same treatment decision for the patient. Finally, it is important to understand whether biomarker data from a diagnostic sample expression profile are clinically relevant following the genetic and phenotypic changes that can occur under the selective pressure of treatment.

We selected the NanoString nCounter expression system to study the MEK (plus associated CRes; ref. 8) and RAS (9) gene signatures. This probe-based technology measures mRNA abundance in low amounts of total RNA without enzyme reactions and subsequent bias, has demonstrated greater sensitivity than microarrays (12), and has demonstrated superior results with archived FFPET specimens compared with RT-qPCR (13). The degree of multiplexing offered by the technology is relevant to our gene signature size; additionally, it has demonstrated potential with gene signatures in several clinical studies (14–16).

Here, we describe the steps taken to convert the published MEK and RAS signatures to a NanoString format consistent with the quantity and quality of tumor tissue specimens routinely available from patients with NSCLC. Furthermore, we systematically addressed technical parameters [e.g., reagent batch variability, limit of detection (LOD), and limit of quantification (LOQ)] and biological variables (studying the association with activating *KRAS* mutations, spatiotemporal variation) necessary for clinical hypothesis testing.

Materials and Methods

Refinement of the MEK signature

A sequential annotation and scoring approach assigned a tissue-specific weighting to each of the original 18 MEK signature genes. For each gene in each tumor tissue type, scores of 0 to 4 were assigned to the following features within NSCLC datasets (17–20): reproducibility of mRNA expression bimodality and intra-signature gene correlation across cell lines and patient samples, predictivity of selumetinib response in cell lines and *in vivo* xenograft models, consistent mRNA expression knockdown following MEK inhibition in cell lines and *in vivo* xenograft models, and predictivity of *KRAS* activation in patient samples. A final score (0 to 4) was assigned, based on rounded mean score for each feature, to select the most important genes in NSCLC.

Bimodality was considered positive if default thresholds were met in >1 dataset using the algorithm BiSep (ref. 21; incorporating the Bimodality Index; ref. 22). Co-regulation was considered positive if the gene in question showed Pearson correlation above a threshold to >4 other signature genes in >1 dataset, with the threshold set at either (0.5 × mean Pearson correlation between probe sets to the same gene for all signature genes) or (median Pearson correlation between all genes in signature) depending on whether data were from the Affymetrix array or RNAseq platform, respectively. Predictivity of drug response was considered positive for a gene if mean expression in sensitive cell lines (<1 μmol/L GI_{50}) was higher than resistant (>5 μmol/L GI_{50}), and all outlier low-expressing samples were resistant. Predictivity of pathway activation was considered positive if, in >1 dataset, mean expression was higher in BRAF V600E or KRAS G12 mutant samples than in wild type, and all outlier low-expressing samples were wild type. Dynamic expression was considered positive if gene expression was reduced by at least 1.5-fold following MEK inhibition in cell lines and/or *in vivo* models.

Affymetrix data

NanoString cell line data were generated and compared with historical Affymetrix data using Pearson correlation (23). For each cell line, 4 μg of total RNA was isolated (RNeasy Mini Kit; QIAGEN) and gene expression was measured using Affymetrix HG U133 Plus 2.0 GeneChip arrays following standard protocol (23, 24). Affymetrix gene expression was quantified by robust multiarray analysis (25), and data collapsed gene-centrically (EntrezID) following probe-set QC (23). Data are available via the Gene Expression Omnibus (26), under accession number GSE57083.

NanoString nCounter codeset design

The codeset was designed by NanoString and comprised 18 MEK functional active signature genes and 13 CRes genes (8). For each gene, three distinct probe pairs were generated. One pair was designed to be as close as possible to the Affymetrix gene probe ID transcript sequences used to generate the preclinical cell line Affymetrix data, while maintaining hybridization functionality (Affymetrix NS Probe). One pair had an identical design across two distinct codesets and was used to test batch reproducibility (Batch Comparison Probe). The remaining pair was designed against any other suitable transcript region of the gene (New Probe). NanoString was only able to generate two specific probes for certain genes (Supplementary Table S1 shows probe designs). The codeset also comprised one probe pair per gene for the 147 genes (RAS signature; 105 up and 42 down; ref. 9). A few were shared across signatures (MEK genes: *DUSP4*, *DUSP6*, *PHLDA1*, *S100A6*, *SERPINB1*, and *ZFP106*; CRes genes: *CD274* and *G0S4*). Seventeen reference genes were included (*ABCF1*, *ACTB*, *ALAS1*, *B2M*, *CLTC*, *G6PD*, *GAPDH*, *GUSB*, *HPRT1*, *LDHA*, *PGK1*, *POLR1B*, *POLR2A*, *RPL19*, *RPLP0*, *TBP*, and *TUBB*). For the complete list of genes, see Supplementary Table S2.

NanoString data analysis and signature scoring

Transcript counts were normalized between samples in a particular study using an in-house built tool (NAPPA, publicly available on the Comprehensive R Archive Network, CRAN, Harbron & Wappett (2014) R package: NAPPA http://CRAN.R-project.org/package=NAPPA). Only sample data with a mean Housekeeper (HK) count greater than 50 were processed. Data were Log_2 transformed after being normalized in two steps: Raw NanoString counts were background adjusted with a Truncated Poisson correction using negative control probes (External RNA Controls Consortium approved designed not to bind with any known organism) followed by a technical normalization using integral positive control spike-ins. Data were then corrected for input amount variation through a Sigmoid shrunken slope normalization step using the GEO mean expression of housekeeping genes. Transcripts were designated as "not detected" if the raw count was less than the average of the negative control raw counts plus two standard deviations.

Signature scores were generated from the normalized Log_2 transformed data as previously described (8, 9).

HK gene expression was analyzed in the study of 50 FFPET NSCLC samples using three alternative sets of housekeepers: all of the proposed genes, a set that removed the bottom five (ranked according to Spearman rank correlation R value of each HK with the mean HK value), and a set that removed the bottom 10 genes.

Analysis of 50 NSCLC FFPET samples into hypothetical treatment groups was performed by setting thresholds of either the 75th percentile of signature scores or by calculating the Youden (27) optimal cutoff for differentiating *KRAS* mutants within the dataset.

Cell line samples

Cell lines were obtained directly from the ATCC (Manassas, VA; http://www.atcc.org/) cell bank and passaged in our laboratory for fewer than 6 months after receipt or resuscitation. Human cell lines were authenticated by ATCC using morphology, karyotyping, and PCR-based approaches to confirm identity and to rule out both intra- and interspecies contamination. A549 cells (*KRAS* mutant) were cultured in DMEM (Sigma-Aldrich) containing 10% FCS (Sigma-Aldrich) and 1% glutamine (Sigma-Aldrich). Calu3 cells (*KRAS* mutation not detected) were grown in EMEM supplemented with 10% FCS (Sigma-Aldrich), 1% NEAA (Sigma-Aldrich), 1% sodium pyruvate, and 1% L-glutamine (Sigma-Aldrich). All other cell lines: NCI-H1563, NCI-H522, NCI-H1437 (*KRAS* mutation not detected); Calu6 and NCI-H460 (*KRAS* mutants) were grown in RPMI 1640 (Sigma-Aldrich) supplemented with 10% FCS (Sigma-Aldrich) and 1% L-glutamine (Sigma-Aldrich). Cell lines were not passaged more than 10 times. All cells were cultured in 5% CO_2 at 37°C.

RNA and DNA extraction

NanoString versus Affymetrix. Lung cancer cell lines A549, Calu3, Calu6, NCI-H1563, and NCI-H522 were cultured to 70% confluence in culture media. Cells were pelleted, snap frozen, and stored at −80°C until extraction. Once thawed on ice, cells were lysed with RPE buffer and homogenized using QIAshredder (QIAGEN) technology. RNA was extracted using the QIAGEN RNeasy Mini Kit according to the RNeasy Mini Handbook (September 2010) protocol for "Purification of Total RNA from Animal Cells using Spin Technology."

Treatment of lung cell lines with MEKi and KRAS siRNA

Calu6, NCI-H1437, and NCI-H460 lung cancer cell lines were seeded in 6-well plates and cultured overnight. Cells were treated for 24 hours with a final concentration of 0.3 μmol/L selumetinib made up in DMSO. For modulation of *KRAS* gene expression, cells were treated with 5 nmol/L of either Silencer SELECT KRAS siRNA (#s7940; Applied Biosystems, Life Technologies) or Silencer Negative control #1 (#4390843; Applied Biosystems) in the presence of Lipofectamine RNAiMAX (Life Technologies). The siRNA/Lipid mix remained on the cells for 48 hours, prior to extraction. Following treatment, cells were washed and lysed in RPE buffer, snap frozen, and stored at −20°C until extraction. Once thawed on ice, lysates were homogenized using QIAshredder (QIAGEN) technology. RNA was extracted using the QIAGEN RNeasy Mini Kit, as described above.

NSCLC FFPET samples

FFPET tumor blocks were sourced from the AstraZeneca Global Biobank, in turn purchased from commercial providers whose practices have been reviewed and approved by AstraZeneca as having been obtained ethically with appropriate donor consent and fulfilling AstraZeneca company policies.

A hematoxylin and eosin section for each block was provided for confirmation of NSCLC diagnosis, and estimation of percentage tumor content was defined by a pathologist; all samples were analyzed regardless of tumor content. Intrapatient tumor score variation was studied using 20 matched primary and intrapulmonary lymph node metastatic NSCLC samples from TriStar Technologies (Rockville, MD; http://tristargroup.us/). Fifty NSCLC FFPET samples from Asterand Bio Europe (Royston, Hertfordshire, UK; http://www.asterandbio.com) were used for all other studies and comprised 24 *KRAS*-mutant samples. Testing and analysis were performed blind to *KRAS* status. Four of the 50 TriStar samples covering a range of tumor NanoString expression scores were used to study the spatial variation of the signature score within tumor. Fresh sections were cut from the top, the bottom, and 50 μm in from the top of each patient tumor block.

KRAS mutation test

KRAS mutation status (mutations in codons 12, 13, and 61) was determined by the cobas *KRAS* Mutation Test using purified DNA according to the manufacturer's standard protocol. Samples were processed on the cobas z 480 Analyzer. Only valid results were reported.

NanoString assays

Purified RNA was diluted in nuclease-free water to 20 ng/μL (added neat if <20 ng/μL stock), making a final assay concentration 100 ng in all studies except for the study to determine the optimal RNA input concentration with 400 ng, 200 ng, 100 ng, 50 ng, and 25 ng RNA derived from a single 5-μm NSCLC FFPET sample and the LOQ study where RNA was diluted 2-fold from 20 to 0.6 ng/μL (final assay concentrations of 100, 25, 12.5, 6.25, and 3.13 ng). RNA was hybridized with reporter and capture probes for 16 to 22 hours at 65°C as per the manufacturer's standard protocol. Samples were loaded onto the nCounter Prep Station, whereby target and probe complexes were isolated onto a cartridge following affinity purification, and then imaged and quantified using the nCounter GEN2 Digital Analyzer.

NSCLC FFPET studies

Tumor FFPET material was macro-dissected from 1 to 2 × 5-μm sections (approximately 1 cm^2 in area) per sample using the QIAGEN RNeasy FFPE Kit following the manufacturer's standard protocol. Tissue for *KRAS* mutation testing tumor was scraped from 1 to 2 × 5-μm sections and DNA extracted using the cobas DNA Sample Prep Kit (Roche Diagnostics). RNA and DNA concentration were quantified using the NanoDrop 2000 instrument.

Results

Refinement of the 18-gene MEK signature to the 6-gene lung-optimized MEK signature

An 18-gene "MEK activation signature" was developed by Dry and colleagues (8) initially in a pan-cancer dataset predominantly comprising lung, colorectal, and melanoma cell lines. Dry and colleagues identified genes demonstrating that expression that was higher (ANOVA FDR <0.05, fold change >1.5) in cell lines sensitive (GI_{50} <1 μmol/L) to the MEKi selumetinib; bimodal expression (clear differential between higher and low expressing samples, defined by BiSEp; ref. 28) across cell lines; bimodal-low expression that was exclusive (Fisher $P < 0.01$) to selumetinib-resistant cell lines (GI_{50} >5 μmol/L), because no drug response would be expected if MEK activity were absent; and co-regulation amongst prioritized genes, measured by Pearson correlation of mRNA expression across the cell lines.

Dry and colleagues (8) also further validated the MEK signature genes to show: reproducible bimodality and correlation in patient tumor samples; presence (higher vs. other samples) of expression in independent cell lines sensitive to multiple MEKi; presence (higher vs. other samples) of expression in cell lines and patient samples with genetic activation of the MEK pathway; and dynamic knockdown of expression upon treatment with a MEKi in lung, melanoma, and colon cancer cell lines of multiple genotypes including *KRAS* mutant (fold change >1.5 per cell; ANOVA P <0.05 across cells).

Because published prioritization was based on pan-cancer data, we aimed to refine the "MEK activation signature" and focus on genes that demonstrated a more robust performance specifically within NSCLC. Using the same tests described and referenced above, we assessed which of the 18 genes maintained these criteria specifically and reproducibly within multiple NSCLC sample sets from cancer cell lines, xenograft/explant models, and patients (8, 17–20, 29). Six genes consistently tested positive in all lung cancer datasets: *PHLDA1*, *SPRY2*, *DUSP6*, *DUSP4*, *ETV4*, and *ETV5*.

Using this lung-optimized MEK signature, we aimed to develop a clinical assay with NanoString nCounter gene expression technology to measure transcription profiles in NSCLC FFPET.

Transfer of the lung-optimized MEK signature to the NanoString platform

The lung-optimized MEK signature comprises only six genes and hence could be more susceptible to changes in methodology than a signature comprising an order of magnitude more genes. Two or three NanoString probes per gene were evaluated and expression was compared with Affymetrix data from lung cancer cell lines with a range of signature scores. Figure 1 shows the correlation plots of historical Affymetrix data and NanoString data for each MEK signature gene using the "Affymetrix NS Probe." Pearson correlation coefficients were r of 0.75 or greater for "Affymetrix NS Probe" data when compared with Affymetrix data, except for *ETV5* (r of 0.67). NanoString data for "Batch Comparison" and "New" probes also correlated well with Affymetrix data, except for *ETV5* (both probes) and *DUSP6* ("Batch Comparison" probe only). *DUSP6*, *ETV5*, and *SPRY2* "Affymetrix NS Probe" data correlated better to Affymetrix data than their other gene probes, whereas *DUSP4*, *ETV4*, and *PHLDA1* gave equivalent or better correlations with Affymetrix data with the "Batch Comparison" and "New" probes (Supplementary Table S3).

Pathway intervention modulates signatures

To investigate the ability of NanoString to detect changes in signature score, we studied the effects of selumetinib, a MEKi, and KRAS siRNA on three lung cancer cell lines (Calu6, NCI-H1437, and NCI-H460). Supplementary Fig. S1 shows the effect of selumetinib (0.3 μmol/L) on the MEK signature expression. Selumetinib was shown to decrease the score of all three cell lines. *KRAS* knockdown with siRNA downregulated baseline gene signature expression in the Calu6 and NCI-H460 lines (both *KRAS* mutant). As expected, there was no downregulation in NCI-H1437, a *KRAS* mutation not detected/MEK1-mutant line that shows *KRAS*-independent MEK1 constitutive activation (30). In contrast, KRAS siRNA more strongly reduced the RAS signature score than the MEK signature score in all except the NCI-H1437 cell line as would be expected if the MEK1 mutation was driving gene expression distal to KRAS.

Development of the NanoString gene expression assay for NSCLC FFPET gene signature analysis

The proposed clinical NanoString gene expression assay described above represents not only a change in the technology platform but also sample-type requirements (i.e., from cell or frozen tumor lysate to FFPET). We tested the performance of the MEK, CRes, and RAS signatures in a sample type and quantity consistent with that available in standard clinical practice. To study the signature's ability to identify *KRAS*-mutant samples, we evaluated 50 NSCLC FFPET samples (48% *KRAS* mutant) using one 5-μm section per tumor. Operators were blinded to *KRAS*

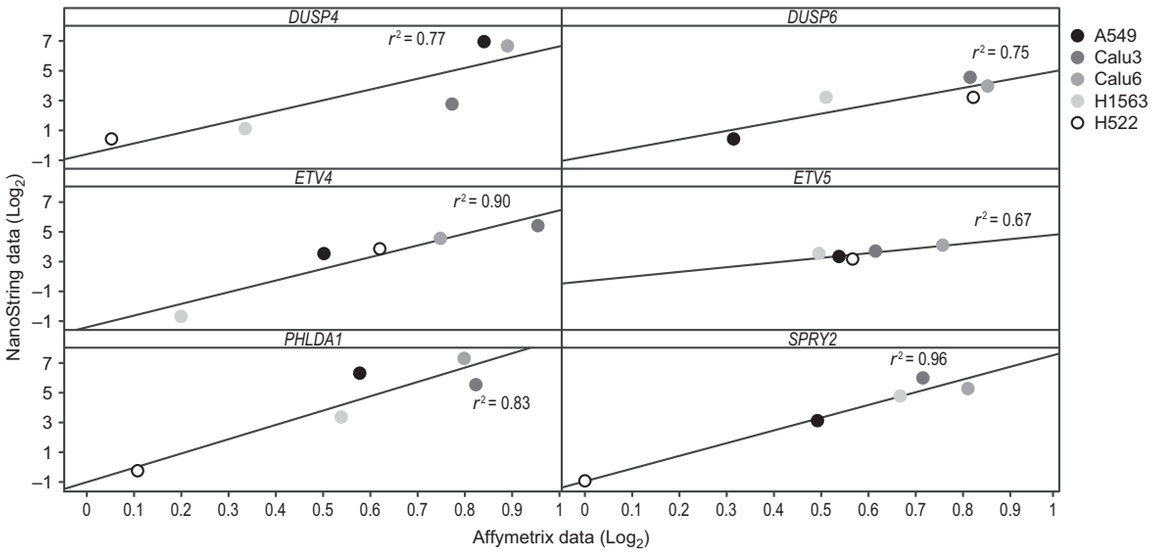

Figure 1.

MEK signature gene expression translates across platforms. NanoString gene expression data (Y-axis) versus Affymetrix gene expression data (X-axis) for individual MEK signature genes (*DUSP4, DUSP6, ETV4, ETV5, PHLDA1*, and *SPRY2*) across lung cell lines A549, Calu3, Calu6, NCI-H1563, and NCI-H522. r^2 = coefficient of determination. NanoString probes were designed to regions covered by the Affymetrix probe sets.

status. Of the 50 FFPET samples, four had lower than the optimum 100 ng of RNA following extraction, and 59 to 97 ng RNA was used in the NanoString assay.

Prior to testing the association between signature output and *KRAS* status, the optimal choice of reference or HK genes and most suitable endogenous gene probes was determined. Suitability of HK genes and stability of expression results were investigated. Testing revealed that almost any variation in the choice of reference genes from the set of 17 HK genes had little impact on the expression patterns of target genes. Analysis of three alternative sets of HKs all showed correlations above 0.95, confirming that the inclusion of all HKs in the analysis was a robust method. HK gene choice is essential in ensuring consistent normalization of sample data and for generating representative expression data prior to scoring.

For the MEK and CRes signatures, gene probe selection was based on interprobe correlations within the 50-sample dataset. For each probe, correlation coefficients were calculated against the other probes, and the probe with the highest average correlation coefficient was chosen to generate MEK and CRes scores (Supplementary Table S4). All genes had a Pearson correlation coefficient $r > 0.8$ where the correlation was the highest between probes (Supplementary Table S4). Supplementary Fig. S2 shows the correlation coefficients for all probes and probes selected for analysis. Further investigation was performed to explore genes where expression was below the LOD. No MEK signature gene expression was below this background level. Out of 13 CRes genes, *STAC* expression was not detected in 13 out of the 50 samples, *IL6* in four samples, and *FZD2* and *CD274* in one sample. Of the 146 RAS signature genes, on average five genes per sample were not detected. One RAS signature gene, *CXCL5*, gave no detectable expression across all 50 samples, highlighting a potential issue with probe design or relevance of the gene in NSCLC. Probes giving below-threshold counts across a number of samples, such as *CXCL5* and *STAC*, were investigated further. A more detailed inspection of the probe design highlighted that many gene probes had been designed to the 3′UTR of the gene, a region that may not be expressed widely in NSCLC. However, low expression could also be biological and not because of probe design. It may be expected that a large gene signature encompassing complex pathway signaling, such as for RAS, would have a high number of samples with one or more genes below the LOD.

The expression range for all of the MEK and CRes genes spanned approximately four logs (Supplementary Fig. S3), suggesting it is acceptable to calculate MEK and CRes signature scores by averaging Log_2-normalized expression data across genes.

Association with *KRAS* status in a blinded study of 50 NSCLC FFPET tumors

Previous work on the 50 NSCLC samples (choice of HK genes, probes for the MEK signature score, and algorithm for MEK signature calculation) was performed blind to *KRAS* status. The results (Fig. 2A) supported observations regarding the association of signature scores with the presence of *KRAS* mutations. Both MEK and RAS signature scores were significantly higher ($P = 0.028$ and 0.003, respectively) in *KRAS*-mutant tumors than in tumors without a detected *KRAS* mutation. Importantly, some tumors without a detected *KRAS* mutation had relatively high signature scores, supporting the hypothesis that MEK or RAS activation is not exclusively linked to *KRAS* mutation and that the signatures may identify tumors with RAS–ERK pathway activation regardless of *KRAS* mutation. Similarly, there are *KRAS*-mutant tumors with signature scores lower than the mean of all 50 scores, suggesting they did not have such a high MEK pathway activation. As expected, the difference between *KRAS*-mutant and *KRAS* mutation not detected signature scores was greater for the RAS signature. Furthermore, when MEK and CRes signature scores were added, the score closely resembled that of the RAS signature

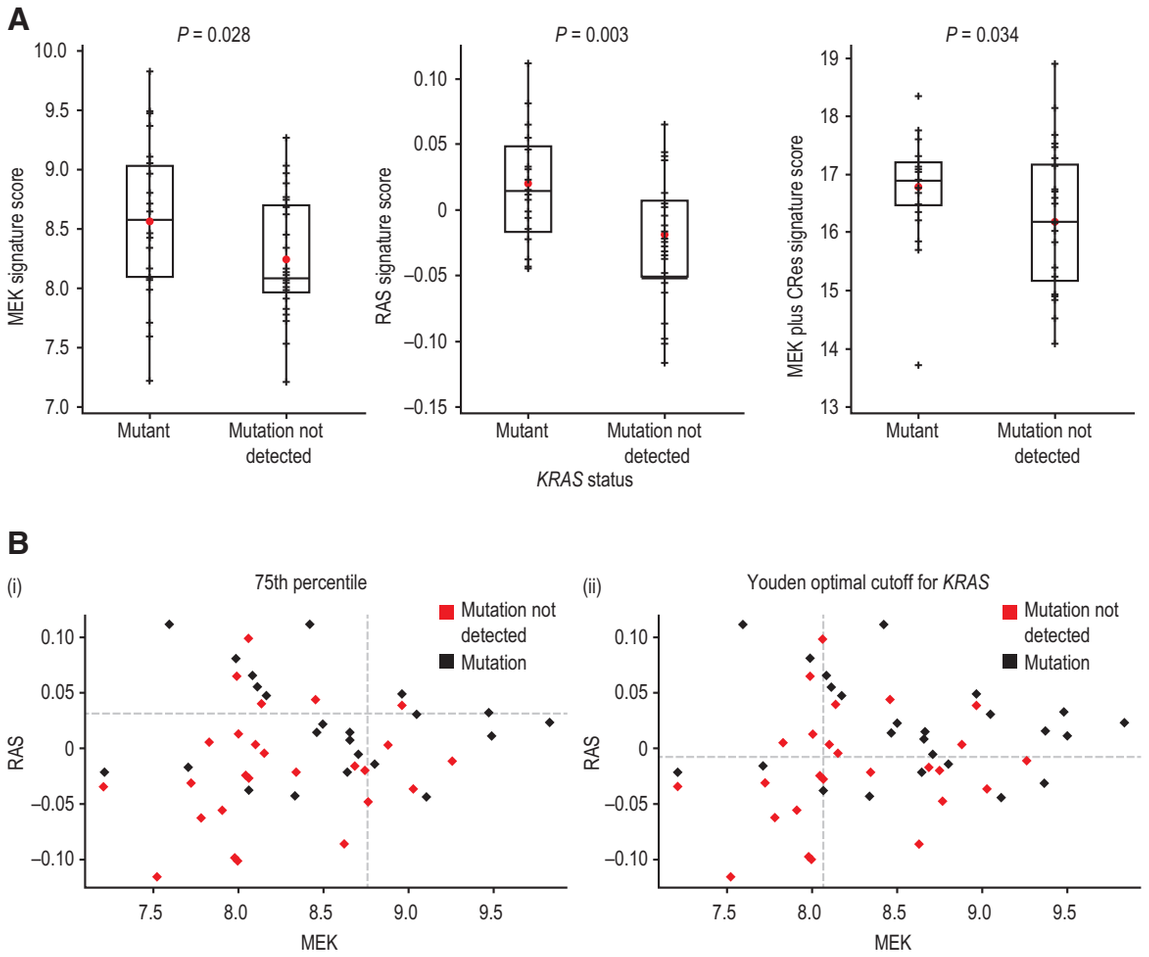

Figure 2.

A, Signature scores are significantly higher in *KRAS*-mutant NSCLC. **B,** MEK signature score defines a different patient population compared with RAS signature and *KRAS* mutation. **A,** The Y-axis shows the MEK, RAS, and MEK plus CRes signature scores in *KRAS*-mutant NSCLC versus mutation not detected. *P* value was generated using a one-sided *t* test. Red spot denotes mean signature score, line within box denotes median score, and outer box edges denote quartile range. **B,** Correlation plots show calculated signature scores for 50 NSCLC samples. (i) 75th percentile value for RAS (Y-axis) and MEK (X-axis) signature scores shown by the dotted line; (ii) Youden cutoff (optimal cutoff that best differentiates between *KRAS* mutation and mutation not detected status) is shown by dotted lines for both signatures. The mutation status of each sample is denoted by color (red, mutation not detected; black, mutation).

(Supplementary Fig. S4), agreeing with the hypothesis that these signatures measure independent components of *KRAS* signaling that is captured in totality when combined.

MEK signature score defines a different patient population compared with RAS signature and *KRAS* mutation

To determine if the signatures and *KRAS* mutation status identified different patient populations, we compared signature scores obtained for the NSCLC samples with and without *KRAS* mutations (Fig. 2B). Patient populations were defined by imposing thresholds of either the 75th percentile of signature scores or by calculating the Youden's J statistic (27). Youden cutoff seeks the optimal cutoff for differentiating *KRAS* mutants within the dataset by calculating the cutoff value that differs maximally from the pure chance line of an ROC curve. Despite both signatures having statistically significant associations with *KRAS* status, there was very little correlation between them (Pearson correlation coefficient $r = 0.016$). This suggests that, in the clinical setting, different patient populations would be eligible for MEKi treatment depending on the biomarker used for patient selection (Fig. 2B). In order to test the association with mutation status, we deliberately chose to analyze a cohort enriched for *KRAS* mutations. Thus, we modeled the impact of signature testing versus mutation testing using the actual prevalence of *KRAS* mutations in NSCLC of approximately 20%. If the decision to treat with a MEKi were based on the MEK cutoff at Youden optimal of 8.072, then the treatment decision could be different for as many as 58% of patients (Table 1); in this example, the 51% of patients with NSCLC without a detected *KRAS* mutation who were MEK pathway activated (MEK-high) would have received a MEKi if the patient selection was by MEK signature profile rather than by *KRAS* mutation status. Likewise,

Table 1. Signature scores and *KRAS* mutation status define different patient populations

	***KRAS*m (%)**	***KRAS* ND (%)**	**Total (%)**
(i)			
MEK-high	**13**	**51**	**64**
MEK-low	7	29	36
Total	20	80	100
Cutoff = 8.072 derived by the Youden method.			
(ii)			
RAS-high	**9**	**35**	**44**
RAS-low	11	45	56
Total	20	80	100
Cutoff = 0.0078 derived by the Youden method.			
(iii)			
MEK-high	**5**	**21**	**26**
MEK-low	15	59	74
Total	20	80	100
Cutoff = 8.762 derived from MEK signature score at the 75th percentile.			
(iv)			
RAS-high	**5**	**21**	**26**
RAS-low	15	59	74
Total	20	80	100
Cutoff = 0.032 derived from RAS signature score at the 75th percentile.			

NOTE: Signature scores were dichotomized using the Youden optimal, (i) and (ii), or 75th percentile, (iii) and (iv). Candidate patients are indicated by underlining (*KRAS* mutated) or bold (signature high or "positive").
Abbreviations: *KRAS*m, *KRAS* mutated; *KRAS* ND, *KRAS* mutation not detected.

the 7% of patients with *KRAS*-mutant NSCLC who were not MEK pathway activated according to MEK signature profile (MEK-low) would have received a MEKi if selection was based on *KRAS* status and not the transcriptional profile. A similar result was shown for the RAS signature; 46% of patients would have received a different treatment decision based on the signature profile results compared with *KRAS* mutation testing result. These data demonstrate that *KRAS* mutation status and MEK gene signature approaches are very different.

Gene expression profiles are maintained at reduced RNA starting concentrations

NSCLC tumor samples are variable in quality and often limited in quantity. Furthermore, RNA extracted from FFPET is notoriously fragmented, which can be challenging for gene expression assays. Hence, it is particularly important to understand the LOD and robustness of the MEK signature to suboptimal amounts of RNA. NanoString nCounter gene expression technology claims superior results with FFPET over other technologies due to direct hybridization of small base-pair probes to mRNA; direct digital counting of hybridized molecular coded mRNA-probe complexes; and lack of enzyme amplification (13).

To define the optimal starting RNA input concentration, we determined the detection level of a large gene panel, including all signature genes, at 400 ng, 200 ng, 100 ng, 50 ng, and 25 ng RNA derived from a single NSCLC FFPET sample. Only one of 460 genes was not detected above background with 100 ng RNA compared with 200 ng and 400 ng input RNA. By contrast, 19 and 50 genes were undetected with 50 ng and 25 ng, respectively. NanoString nCounter assays require 5 μL of total RNA at 20 ng/μL to add 100 ng. The concentration of RNA extracted from this sample was 95 ng/μL in 26 μL total volume; thus, 100 ng was considered optimal for NSCLC studies.

We examined the ability to reduce RNA input concentrations using samples at a range of signature scores. Samples were serially diluted 2-fold from 100 ng RNA to 3.13 ng, and scores calculated. Signatures were relatively consistent down to 25 ng for all samples (Fig. 3), suggesting that clinical samples yielding suboptimal RNA quantities generate reliable signature scores. In addition, the LOD was studied with a predetermined "low" score sample (data not shown). MEK signature genes were expressed above the LOD in all but the lowest RNA concentration, where two of the six genes were not detected. Of the 147 RAS signature genes, the number detected below the LOD increased with decreasing RNA input; concentrations of RNA 100, 50, 25, 12.5, 6.25, and 3.13 ng gave 0 (0%), 5 (3.4%), 13 (8.9%), 21 (14.4%), 31 (21.2%), and 40 (27.4%) undetected RAS signature genes, respectively. Overall, the results

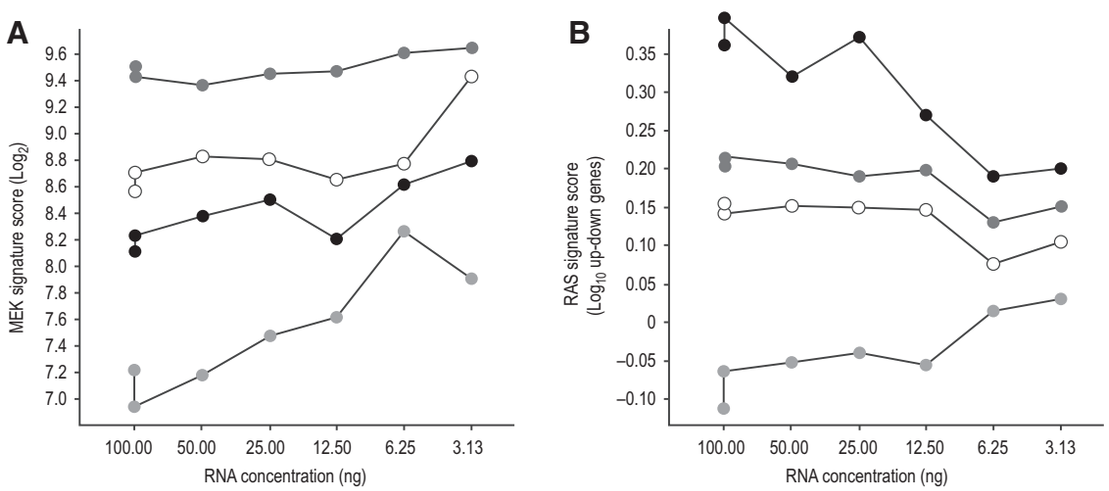

Figure 3.
Signature scores remain consistent with 4-fold less RNA starting material. MEK (**A**) and RAS (**B**) signature scores (Y-axis) relative to the concentration of RNA (ng) added to NanoString assays (X-axis). Four NSCLC samples retrospectively selected based on their RAS and MEK signature score are represented by shading: black, high RAS; dark gray, high MEK; white, medium MEK/medium RAS; light gray, low MEK/low RAS. Technical repeat of data of samples added at 100 ng RNA is shown.

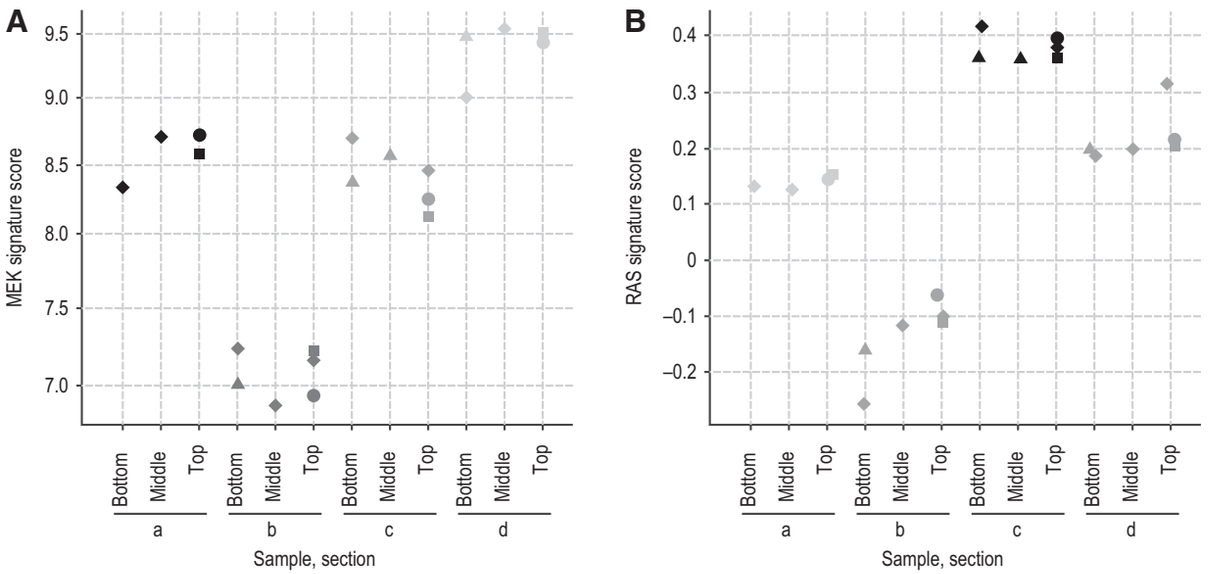

Figure 4.

Spatial conservation of signature scores in NSCLC tumors. The Y-axis shows the MEK (**A**) and RAS signature scores (**B**) of four NSCLC FFPET samples (a, b, c, and d) from sections cut from the top, middle, and bottom of each block (X-axis). Shapes represent separate NanoString runs. Data annotated as squares and circles originate from the same extracted batch of RNA, as is the case with triangles and diamonds.

demonstrate that the assay is robust and that scores are conserved when suboptimal amounts of RNA are assayed.

We also examined the reproducibility of expression measured by the NanoString assay upon repeat testing with a different manufacturing batch of probes. MEK signature gene probes (18 original genes) from two different batches were compared using an FFPET NSCLC sample at RNA concentrations of 200 ng, 100 ng, 50 ng, and 25 ng. Pearson correlations showed a high agreement of expression across all RNA amounts giving *r* values of 0.97, 0.94, 0.92, and 0.75, respectively (Supplementary Fig. S5).

Spatial and temporal conservation of signature scores in NSCLC tumors

For a gene signature to have clinical utility as a biomarker assay, intrapatient variability needs to be lower than interpatient variability. We studied four NSCLC FFPET samples and compared the MEK and RAS gene expression profiles across different sections throughout the same patient tumor. Samples were selected on their previous MEK or RAS signature score (i.e., low, medium, or high scores). Tumor blocks were sectioned from the top, 50 μmol/L from the top (middle), and from the bottom. Figure 4A shows that MEK signature scores were conserved throughout the tumor. Additionally, technical replicates across all sections of the same tumor were comparable. Similar results were shown for the RAS signature scores (Fig. 4B).

An important, yet frequently untested, assumption is that biomarker data derived from diagnostic tumor samples are sufficiently relevant to direct the treatment of subsequent disease. The assumption can be tested by examining the longitudinal concordance of assay results and tumor biology. We tested the hypothesis that gene signature scores would be conserved between primary and metastatic disease and that this would be maintained regardless of *KRAS* mutation status. MEK signature scores were conserved across primary and metastatic tumor from 20 patients (Fig. 5A). Statistical analysis confirmed the variability in the signature profiles between patients was nearly 3-fold greater than the variability between primary and metastatic tumor of the same patient. Similar results were achieved for RAS signature but with a 3.5-fold difference in the variability (Fig. 5B).

Discussion

NanoString nCounter technology provides a means to test the prognostic and predictive capabilities of gene expression signatures in NSCLC FFPET. We developed a clinically relevant, robust NanoString assay using a lung-optimized gene signature to measure MEK pathway output in NSCLC.

Our six-gene lung-optimized MEK signature was developed using the process and criteria described by Dry and colleagues (8). We transferred the lung-optimized MEK signature to the NanoString platform and demonstrated that signature gene expression was robust across both the Affymetrix and NanoString platforms. Moreover, the majority of the NanoString probes were successful in measuring their target gene in cell lines.

We investigated the ability of NanoString to detect changes in signature score by studying the effects of selumetinib and *KRAS* siRNA on three lung cancer cell lines. The differential effects we observed with *KRAS* siRNA on the cell lines support the six-gene signature's postulated ability to measure MEK pathway output when assayed on the NanoString and that the MEK signature is more specific to MEK signaling than the RAS signature.

Subsequently, we tested the NanoString gene expression assay in FFPET samples that were consistent with those available in standard clinical practice. We determined which HK genes to use for data normalization, selected the most suitable MEK and CRes probes, and showed detectable MEK signature genes expression in

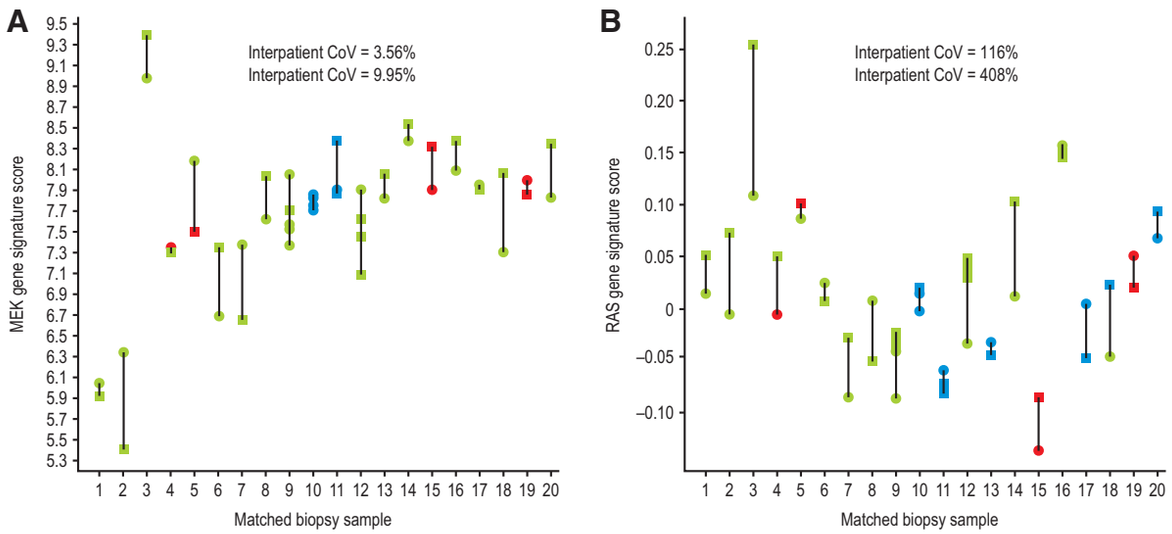

Figure 5.

Temporal conservation of signature scores in NSCLC tumors. MEK (**A**) and RAS (**B**) signature scores (Y-axis) of primary tumor tissue (circles) compared with metastatic tumor tissue (squares) of 20 paired biopsy NSCLC samples (X-axis). Samples are colored by *KRAS* status: blue, no mutation data; red, *KRAS* mutant; green, *KRAS* mutation not detected. Two paired samples showed differences in *KRAS* status. Repeat test of RNA was performed for some samples. For each patient, intrapatient coefficient of variation (CoV) was calculated with formula: $SD_{patient}/Ave_{patient} \times 100$. The average intrapatient CoV was then calculated. Interpatient CoV was calculated with: $SD(Ave_{patient})/Ave(Ave_{patient}) \times 100$. Variability in MEK signature score between patients is 2.8-fold greater than the variability between primary and metastatic tumor of the same patients. Variability in RAS signature score between primary and metastatic tumor of the same patients is 3.5-fold less than the variability in signature between patients.

all samples and measurable RAS signature expression for the majority of genes in most samples. The optimized probe selection and HK genes were incorporated into the analysis and used for the calculation of signature scores.

Calculating the MEK and CRes signature scores by averaging Log_2-normalized expression data across genes was deemed acceptable, as the expression range for all of the MEK and CRes genes spanned approximately four logs. If, however, the dynamic range of expression varied greatly for some but not all genes, this could skew the score and, with our method of calculation, not accurately represent the pathway activation status. This was not a concern with RAS signature analysis, because scores were calculated by taking away the mean of "downregulated genes" from mean of "upregulated" genes (regulated up or down in response to RAS pathway output increases; ref. 9).

NSCLC tumor samples are frequently variable in quality and limited in quantity. Thus, we investigated the LOD and robustness of the MEK signature to suboptimal amounts of RNA. Our results showed that gene expression profiles were maintained at reduced RNA starting concentrations, and we concluded that 100-ng RNA in a single NSCLC FFPET sample was optimal for NSCLC studies.

Furthermore, we demonstrated that the signature assay is remarkably conserved within and between tumors, meeting the prerequisites of a predictive tumor marker as described by Hodgson and colleagues (31). Our data suggest that RAS–ERK biology is conserved despite disease progression and that signature analysis has the potential to direct treatment decisions for patients with both primary and metastatic NSCLC tumors. Additionally, the data demonstrate maintenance of the signature profiles despite tumor stage and regardless of *KRAS* status of the primary tumor.

A clear role for *KRAS* testing in selecting patients for treatment with a MEKi has not been conclusively demonstrated (3, 4). Although we confirmed the association between MEK signatures and *KRAS* mutation status in NSCLC, our data clearly show that if such signatures can capture the dependence of tumors on MEK signaling, then the sensitivity and specificity of *KRAS* testing for MEKi treatment decisions could be improved upon. Although the ability of either approach to select lung cancer patients who will respond to MEKi remains to be tested in the clinic, high MEK signature scores have recently been associated with response to MEKi/taxane, but not taxane alone, in a blinded analysis of a clinical trial in *BRAF* wild-type cutaneous melanoma (32), and the MEK signature is being used to prospectively test patients for inclusion in a MEKi/taxane combination trial in gastric cancer (https://clinicaltrials.gov/ct2/show/NCT02448290).

In conclusion, we developed a technically and biologically robust NanoString gene expression assay of MEK pathway output, compatible with the quantities of FFPET routinely available. The gene signatures identified a different patient population for MEK inhibitor treatment compared with *KRAS* mutation testing. The predictive power of the MEK signature should be studied and further refined in clinical trials.

Disclosure of Potential Conflicts of Interest

E.A. Harrington, P.D. Smith, and D. Hodgson hold ownership interest (including patents) in AstraZeneca. No potential conflicts of interest were disclosed by the other authors.

Authors' Contributions

Conception and design: R. Brant, A. Sharpe, J.R. Dry, E.A. Harrington, J.C. Barrett, P. Smith, D.R. Hodgson

Development of methodology: R. Brant, A. Sharpe, T. Liptrot, J.R. Dry, E.A. Harrington, J.C. Barrett, D.R. Hodgson
Acquisition of data (provided animals, acquired and managed patients, provided facilities, etc.): R. Brant, J.C. Barrett, N. Whalley, C. Womack
Analysis and interpretation of data (e.g., statistical analysis, biostatistics, computational analysis): R. Brant, A. Sharpe, T. Liptrot, J.R. Dry, E.A. Harrington, J.C. Barrett, C. Womack, P. Smith, D.R. Hodgson
Writing, review, and/or revision of the manuscript: R. Brant, A. Sharpe, J.R. Dry, E.A. Harrington, J.C. Barrett, C. Womack, P. Smith, D.R. Hodgson
Administrative, technical, or material support (i.e., reporting or organizing data, constructing databases): R. Brant
Study supervision: R. Brant, E.A. Harrington, J.C. Barrett, D.R. Hodgson

Acknowledgments

Thanks to the selumetinib team and Gayle Marshall of AstraZeneca for providing scientific guidance. Technical editing assistance was provided by Lucy Turner of iMed Comms, Macclesfield, UK.

Grant Support

This research was funded by AstraZeneca.

The costs of publication of this article were defrayed in part by the payment of page charges. This article must therefore be hereby marked *advertisement* in accordance with 18 U.S.C. Section 1734 solely to indicate this fact.

Received January 6, 2016; revised September 14, 2016; accepted September 27, 2016; published OnlineFirst October 12, 2016.

References

1. Dogan S, Shen R, Ang DC, Johnson ML, D'Angelo SP, Paik PK, et al. Molecular epidemiology of EGFR and KRAS mutations in 3,026 lung adenocarcinomas: higher susceptibility of women to smoking-related KRAS-mutant cancers. Clin Cancer Res 2012;18:6169–77.
2. Dearden S, Stevens J, Wu YL, Blowers D. Mutation incidence and coincidence in non–small-cell lung cancer: meta-analyses by ethnicity and histology (mutMap). Ann Oncol 2013;24:2371–6.
3. Guan JL, Zhong WZ, An SJ, Yang JJ, Su J, Chen ZH, et al. KRAS mutation in patients with lung cancer: a predictor for poor prognosis but not for EGFR-TKIs or chemotherapy. Ann Surg Oncol 2013;20:1381–8.
4. Roberts PJ, Stinchcombe TE. KRAS mutation: should we test for it, and does it matter? J Clin Oncol 2013;31:1112–21.
5. Janne PA, Shaw AT, Pereira JR, Jeannin G, Vansteenkiste J, Barrios C, et al. Selumetinib plus docetaxel for KRAS-mutant advanced non-small-cell lung cancer: a randomised, multicentre, placebo-controlled, phase 2 study. Lancet Oncol 2013;14:38–47.
6. Gandara DR, Hiret S, Blumenschein GR, Barlesi F, Delord J-R, Madelaine J, et al. Oral MEK1/MEK2 inhibitor trametinib (GSK1120212) in combination with docetaxel in KRAS-mutant and wild-type (WT) advanced non-small cell lung cancer (NSCLC): a phase I/Ib trial. J Clin Oncol 31, 2013 (suppl; abstr 8028).
7. Downward J. Targeting RAS signalling pathways in cancer therapy. Nat Rev Cancer 2003;3:11–22.
8. Dry JR, Pavey S, Pratilas CA, Harbron C, Runswick S, Hodgson D, et al. Transcriptional pathway signatures predict MEK addiction and response to selumetinib (AZD6244). Cancer Res 2010;70:2264–73.
9. Loboda A, Nebozhyn M, Klinghoffer R, Frazier J, Chastain M, Arthur W, et al. A gene expression signature of RAS pathway dependence predicts response to PI3K and RAS pathway inhibitors and expands the population of RAS pathway activated tumors. BMC Med Genom 2010;3:26.
10. Ramaswamy S. Translating cancer genomics into clinical oncology. N Engl J Med 2004;350:1814–6.
11. Sotiriou C, Piccart MJ. Taking gene-expression profiling to the clinic: when will molecular signatures become relevant to patient care? Nat Rev Cancer 2007;7:545–53.
12. Geiss GK, Bumgarner RE, Birditt B, Dahl T, Dowidar N, Dunaway DL, et al. Direct multiplexed measurement of gene expression with color-coded probe pairs. Nat Biotechnol 2008;26:317–25.
13. Reis PP, Waldron L, Goswami RS, Xu W, Xuan Y, Perez-Ordonez B, et al. mRNA transcript quantification in archival samples using multiplexed, color-coded probes. BMC Biotechnol 2011;11:46.
14. Golub TR, Slonim DK, Tamayo P, Huard C, Gaasenbeek M, Mesirov JP, et al. Molecular classification of cancer: class discovery and class prediction by gene expression monitoring. Science 1999;286:531–7.
15. van 't Veer LJ, Dai H, van de Vijver MJ, He YD, Hart AA, Mao M, et al. Gene expression profiling predicts clinical outcome of breast cancer. Nature 2002;415:530–6.
16. van de Vijver MJ, He YD, van 't Veer LJ, Dai H, Hart AA, Voskuil DW, et al. A gene-expression signature as a predictor of survival in breast cancer. N Engl J Med 2002;347:1999–2009.
17. Bild AH, Yao G, Chang JT, Wang Q, Potti A, Chasse D, et al. Oncogenic pathway signatures in human cancers as a guide to targeted therapies. Nature 2006;439:353–7.
18. Cancer Genome Atlas Research Network. Comprehensive genomic characterization of squamous cell lung cancers. Nature 2012;489:519–25.
19. Cancer Genome Atlas Research Network. Comprehensive molecular profiling of lung adenocarcinoma. Nature 2014;511:543–50.
20. Ding L, Getz G, Wheeler DA, Mardis ER, McLellan MD, Cibulskis K, et al. Somatic mutations affect key pathways in lung adenocarcinoma. Nature 2008;455:1069–75.
21. Wappett M. Package `BiSEp'. 2015.
22. Wang J, Wen S, Symmans WF, Pusztai L, Coombes KR. The bimodality index: a criterion for discovering and ranking bimodal signatures from cancer gene expression profiling data. Cancer Informatics 2009;7:199–216.
23. Kim K, Infante J, Cohen R, Burris H, Emeribe U, Curt G, et al. A phase I dose-escalation study of selumetinib in combination with docetaxel in patients with advanced solid tumors [abstract]. In: Proceedings of the AACR-NCI-EORTC International Conference: Molecular Targets and Cancer Therapeutics; 2011 Nov 12–16; San Francisco, CA. Philadelphia (PA): AACR; Mol Cancer Ther 2011;10(11 Suppl):Abstract nr B225.
24. Functional Genomics Data Society (FGED). MIAME: Minimum Information About a Microarray Experiment. Available athttp://fged.org/projects/miame/(accessed December 9, 2015).
25. McCall MN, Bolstad BM, Irizarry RA. Frozen robust multiarray analysis (fRMA). Biostatistics 2010;11:242–53.
26. Messersmith WA, Hidalgo M, Carducci M, Eckhardt SG. Novel targets in solid tumors: MEK inhibitors. Clin Adv Hematol Oncol 2006;4:831–6.
27. Youden WJ. Index for rating diagnostic tests. Cancer 1950;3:32–5.
28. Wappett M, Dulak A, Yang ZR, Al-Watban A, Bradford J, Dry JR. Multi-omic measurement of mutually exclusive loss-of-function enriches for candidate synthetic lethal gene pairs. BMC Genomics 2016;17:65.
29. Pratilas CA, Hanrahan AJ, Halilovic E, Persaud Y, Soh J, Chitale D, et al. Genetic predictors of MEK dependence in non-small cell lung cancer. Cancer Res 2008;68:9375–83.
30. Marks JL, Gong Y, Chitale D, Golas B, McLellan MD, Kasai Y, et al. Novel MEK1 mutation identified by mutational analysis of epidermal growth factor receptor signaling pathway genes in lung adenocarcinoma. Cancer Res 2008;68:5524–8.
31. Hodgson DR, Whittaker RD, Herath A, Amakye D, Clack G. Biomarkers in oncology drug development. Mol Oncol 2009;3:24–32.
32. Gupta A, Brant R, Asher R, Sharpe A, Hodgson D, Love S, et al. Predicting response to MEK inhibitor and chemotherapy combination treatment in BRAF wild-type melanoma using gene expression analysis [abstract]. In: Proceedings of the 10th NCRI Cancer Conference; 2014 Nov 2–5; Liverpool, UK. London (UK): National Cancer Research Institute (NCRI); 2014. Abstract nr B64.